

# Are $\eta$ - and $\omega$ -nuclear states bound ?

K. Tsushima <sup>\*</sup>, D.H. Lu <sup>†</sup>, A.W. Thomas <sup>‡</sup>

Special Research Center for the Subatomic Structure of Matter

and Department of Physics and Mathematical Physics

The University of Adelaide, SA 5005, Australia

K. Saito <sup>§</sup>

Physics Division, Tohoku College of Pharmacy

Sendai 981-8558, Japan

## Abstract

We investigate theoretically whether it is feasible to detect  $\eta$ - and  $\omega$ -nucleus bound states. As well as the closed shell nuclei,  $^{16}\text{O}$ ,  $^{40}\text{Ca}$ ,  $^{90}\text{Zr}$  and  $^{208}\text{Pb}$ , we also investigate  $^6\text{He}$ ,  $^{11}\text{B}$  and  $^{26}\text{Mg}$ , which are the final nuclei in the proposed experiment involving the  $(d, ^3\text{He})$  reaction at GSI. Potentials for the  $\eta$  and  $\omega$  mesons in these nuclei are calculated in local density approximation, embedding the mesons in the nucleus described by solving the mean-field equations of motion in the QMC model. Our results suggest that one should expect to find  $\eta$ - and  $\omega$ -nucleus bound states in all these nuclei.

*PACS:* 36.10.G, 14.40, 12.39.B, 21.65, 71.25

*Keywords:* Meson-nucleus bound states, Quark-meson coupling model, In-medium meson properties, MIT bag model, Effective mass

---

<sup>\*</sup>ktsushim@physics.adelaide.edu.au

<sup>†</sup>dlu@physics.adelaide.edu.au

<sup>‡</sup>athomas@physics.adelaide.edu.au

<sup>§</sup>ksaito@nucl.phys.tohoku.ac.jp

The study of the properties of hadrons in a hot and/or dense nuclear medium is one of the most exciting new directions in nuclear physics. In particular, the medium modification of the light vector ( $\rho$ ,  $\omega$  and  $\phi$ ) meson masses has been investigated extensively by many authors [1]. It has been suggested that dilepton production in the nuclear medium formed in relativistic heavy ion collisions, can provide a unique tool to measure such modifications as meson mass shifts. For example, the experimental data obtained at the CERN/SPS by the CERES [2] and HELIOS [3] collaborations has been interpreted as evidence for a downward shift of the  $\rho$  meson mass in dense nuclear matter [4]. To draw a more definite conclusion, measurements of the dilepton spectrum from vector mesons produced in nuclei are planned at TJNAF [5] and GSI [6]

Recently, a new, alternative approach to study meson mass shifts in nuclei was suggested by Hayano *et al.* [7]. Their suggestion is to use the (d,  $^3\text{He}$ ) reaction to produce  $\eta$  and  $\omega$  mesons with nearly zero recoil. If the meson feels a large enough, attractive (scalar) force inside a nucleus, the meson is expected to form meson-nucleus bound states. Hayano *et al.* [8] have estimated the binding energies for various  $\eta$ -mesic nuclei. They have also calculated some quantities for the  $\omega$  meson case. However, they used an  $\eta$ -nucleus optical potential calculated to first-order in density, taking as input the  $\eta$ -nucleon scattering length. In this article, we use an alternative, self-consistent method to study whether it is possible to form  $\eta$ - and  $\omega$ -nucleus bound states in  $^{16}\text{O}$ ,  $^{40}\text{Ca}$ ,  $^{90}\text{Zr}$  and  $^{208}\text{Pb}$ , as well as  $^6\text{He}$ ,  $^{11}\text{B}$  and  $^{26}\text{Mg}$ . The latter three nuclei correspond to the proposed experiments at GSI [7] using the (d, $^3\text{He}$ ) reaction – i.e., the reactions,  $^7\text{Li}(\text{d},^3\text{He})^6_{\eta/\omega}\text{He}$ ,  $^{12}\text{C}(\text{d},^3\text{He})^{11}_{\eta/\omega}\text{B}$  and  $^{27}\text{Al}(\text{d},^3\text{He})^{26}_{\eta/\omega}\text{Mg}$ .

In earlier work we addressed the question of whether quarks play an important role in finite nuclei [9, 10, 11]. The quark-meson coupling (QMC) model [12, 9], which is based explicitly on quark degrees of freedom, is probably one of the most appropriate models to study whether meson-nucleus bound states are possible. The model has been able to describe successfully the static properties of both nuclear matter and finite nuclei [10, 13], as well as meson properties in the nuclear medium [11]. Thus, the model is ideally suited to treat a bound meson and the nucleons in a nucleus on the same footing. In this study, we investigate the possible formation of the  $\eta$ - and  $\omega$ -nucleus bound states due to downward shifts of the masses. We will use QMC-I [11], where the effective, isoscalar-vector  $\omega$  field, which is off mass-shell and mediates the

interactions among nucleons, is distinguished from the physical (on mass-shell)  $\omega$  meson which is produced inside the nuclei by the above mentioned experiments.

One of the most attractive features of QMC is that, in practice, it is not significantly more complicated than Quantum Hadrodynamics (QHD) [14], although the quark substructure of hadrons is explicitly implemented. Furthermore, it produces a reasonable value for the nuclear incompressibility. A detailed description of the Lagrangian density, and the mean-field equations of motion needed to describe a finite nucleus, is given in Refs. [9, 10, 11].

At position  $\vec{r}$  in a nucleus (the coordinate origin is taken at the center of the nucleus), the Dirac equations for the quarks and antiquarks in the  $\eta$  and  $\omega$  meson bags are given by [11]:

$$\left[ i\gamma \cdot \partial_x - (m_q - V_\sigma(\vec{r})) \mp \gamma^0 \left( V_\omega(\vec{r}) + \frac{1}{2} V_\rho(\vec{r}) \right) \right] \begin{pmatrix} \psi_u(x) \\ \psi_{\bar{u}}(x) \end{pmatrix} = 0, \quad (1)$$

$$\left[ i\gamma \cdot \partial_x - (m_q - V_\sigma(\vec{r})) \mp \gamma^0 \left( V_\omega(\vec{r}) - \frac{1}{2} V_\rho(\vec{r}) \right) \right] \begin{pmatrix} \psi_d(x) \\ \psi_{\bar{d}}(x) \end{pmatrix} = 0, \quad (2)$$

$$[i\gamma \cdot \partial_x - m_s] \psi_s(x) \text{ (or } \psi_{\bar{s}}(x)) = 0. \quad (3)$$

(Note that we have neglected a possible, very slight variation of the scalar and vector mean-fields inside the meson bag due to its finite size [9].) The mean-field potentials for a bag centered at position  $\vec{r}$  in the nucleus, which will be calculated self-consistently, are defined by,  $V_\sigma(\vec{r}) = g_\sigma^q \sigma(\vec{r})$ ,  $V_\omega(\vec{r}) = g_\omega^q \omega(\vec{r})$  and  $V_\rho(\vec{r}) = g_\rho^q b(\vec{r})$ , with  $g_\sigma^q, g_\omega^q$  and  $g_\rho^q$  being, respectively, the corresponding quark and meson-field coupling constants. Here we assume that the current masses are given as  $m_q \equiv m_u = m_d = m_{\bar{u}} = m_{\bar{d}}$ . Furthermore, we have assumed that the  $\sigma$ ,  $\omega$  and  $\rho$  fields only interact directly with the nonstrange quarks and antiquarks [11]. The mean meson fields at position  $\vec{r}$  in the nucleus are calculated self-consistently by solving Eqs. (23) – (30) of Ref. [10].

Hereafter we use the notation,  $\omega_B$ , to specify the physical, bound  $\omega$  meson, in order to avoid confusion with the isoscalar-vector  $\omega$  field appearing in QMC. The static solution for the ground state quarks or antiquarks in the  $\eta$  and  $\omega$  meson bags may be written as:

$$\psi_f(x) = N_f e^{-i\epsilon_f t / R_j^*} \psi_f(\vec{x}), \quad (\text{for } j = \eta, \omega_B \text{ and } f = u, \bar{u}, d, \bar{d}, s, \bar{s}), \quad (4)$$

where  $N_f$  and  $\psi_f(\vec{x})$  are respectively the normalization factor and corresponding spin and spatial part of the wave function [11]. The bag radius in medium,  $R_j^*$  ( $j = \eta, \omega_B$ ), which

depends on the hadron species in which the quarks and antiquarks belong, will be determined self-consistently through the stability condition for the (in-medium) mass of the meson against the variation of the bag radius. (See Eq. (10) below.) The eigenenergies for the quarks, in units of  $1/R_j^*$ , are given by

$$\begin{aligned} \begin{pmatrix} \epsilon_u(\vec{r}) \\ \epsilon_{\bar{u}}(\vec{r}) \end{pmatrix} &= \Omega_q^*(\vec{r}) \pm R_j^* \left( V_\omega(\vec{r}) + \frac{1}{2} V_\rho(\vec{r}) \right), \\ \begin{pmatrix} \epsilon_d(\vec{r}) \\ \epsilon_{\bar{d}}(\vec{r}) \end{pmatrix} &= \Omega_q^*(\vec{r}) \pm R_j^* \left( V_\omega(\vec{r}) - \frac{1}{2} V_\rho(\vec{r}) \right), \\ \epsilon_s(\vec{r}) &= \epsilon_{\bar{s}}(\vec{r}) = \Omega_s(\vec{r}), \end{aligned} \quad (5)$$

where  $\Omega_q^*(\vec{r}) = \sqrt{x_q^2 + (R_j^* m_q^*)^2}$  and  $\Omega_s(\vec{r}) = \sqrt{x_s^2 + (R_j^* m_s)^2}$  with  $m_q^* = m_q - g_\sigma^q \sigma(\vec{r})$  ( $q = u, \bar{u}, d, \bar{d}$ ). The bag eigenfrequencies,  $x_q$  and  $x_s$ , are determined by the usual, linear boundary condition [9].

Next, we consider the  $\eta$  and  $\omega_B$  meson masses in the nucleus. The physical states of the  $\eta$  and  $\omega_B$  mesons are the superpositions of the octet and singlet states:

$$\xi = \xi_8 \cos \theta_{P,V} - \xi_1 \sin \theta_{P,V}, \quad \xi' = \xi_8 \sin \theta_{P,V} + \xi_1 \cos \theta_{P,V}, \quad (6)$$

with

$$\xi_1 = \frac{1}{\sqrt{3}} (u\bar{u} + d\bar{d} + s\bar{s}), \quad \xi_8 = \frac{1}{\sqrt{6}} (u\bar{u} + d\bar{d} - 2s\bar{s}), \quad (7)$$

where  $(\xi, \xi')$  denotes  $(\eta, \eta')$  or  $(\phi, \omega_B)$ , with the mixing angles  $\theta_P$  or  $\theta_V$ , respectively [15]. Then, the masses for the  $\eta$  and  $\omega_B$  mesons in the nucleus at the position  $\vec{r}$ , are self-consistently calculated by:

$$m_\eta^*(\vec{r}) = \frac{2[a_P^2 \Omega_q^*(\vec{r}) + b_P^2 \Omega_s(\vec{r})] - z_\eta}{R_\eta^*} + \frac{4}{3} \pi R_\eta^{*3} B, \quad (8)$$

$$m_{\omega_B}^*(\vec{r}) = \frac{2[a_V^2 \Omega_q^*(\vec{r}) + b_V^2 \Omega_s(\vec{r})] - z_{\omega_B}}{R_{\omega_B}^*} + \frac{4}{3} \pi R_{\omega_B}^{*3} B, \quad (9)$$

$$\left. \frac{\partial m_j^*(\vec{r})}{\partial R_j} \right|_{R_j=R_j^*} = 0, \quad (j = \eta, \omega_B), \quad (10)$$

with

$$a_{P,V} = \frac{1}{\sqrt{3}} \cos \theta_{P,V} - \sqrt{\frac{2}{3}} \sin \theta_{P,V}, \quad b_{P,V} = \sqrt{\frac{2}{3}} \cos \theta_{P,V} + \frac{1}{\sqrt{3}} \sin \theta_{P,V}. \quad (11)$$

In practice, we use  $\theta_P = -10^\circ$  and  $\theta_V = 39^\circ$  [15], neglecting any possible mass dependence and imaginary parts. We also assume that the values of the mixing angles do not change in

medium, although this is possible and merits further investigation. In Eqs. (8) and (9),  $z_\eta$  and  $z_{\omega_B}$  parameterize the sum of the center-of-mass and gluon fluctuation effects, and are assumed to be independent of density [9].

In this study, we chose  $m_q = 5$  MeV and  $m_s = 250$  MeV, for the current quark masses, and  $R_N = 0.8$  fm for the bag radius of the nucleon in free space. Other inputs, parameters, and some of the quantities calculated in the present study, are listed in Table 1. The coupling constants,  $g_\sigma^q$ ,  $g_\omega^q$  and  $g_\rho^q$ , are adjusted to fit the saturation energy and density of symmetric nuclear matter and the bulk symmetry energy. Note that none of the results for nuclear properties depend strongly on the choice of the other parameters – for example, the relatively weak dependence of the final results on the values of the current quark mass and bag radius is shown explicitly in Refs. [9, 10]. The parameters at the hadronic level associated with the core nucleus are summarized in Table 2. The value of the  $\sigma$  mass for finite nuclei is obtained by fitting the r.m.s. charge radius of  $^{40}\text{Ca}$  to the experimental value,  $r_{\text{ch}}(^{40}\text{Ca}) = 3.48$  fm [10]. For more details and explanations of the model parameters, see Refs. [9, 10].

Table 1: Physical masses fitted in free space, free space full widths,  $\Gamma$ , the bag parameters,  $z$ , and the bag radii in free space,  $R$ . The quantities with an asterisk, are those quantities calculated at normal nuclear matter density,  $\rho_0 = 0.15$  fm $^{-3}$ . They are obtained with the bag constant,  $B = (170 \text{ MeV})^4$ , current quark masses,  $m_u = m_d = 5$  MeV and  $m_s = 250$  MeV. Note that the free space width of the  $\eta$  meson is 1.18 keV [15].

	mass (MeV)	$\Gamma$ (MeV)	$z$	$R$ (fm)	$m^*$ (MeV)	$R^*$ (fm)
$N$	939.0 (input)	—	3.295	0.800 (input)	754.5	0.786
$\eta$	547.5 (input)	0 (input)	3.131	0.603	483.9	0.600
$\omega_B$	781.9 (input)	8.43 (input)	1.866	0.753	658.7	0.749

Through Eqs. (1) – (11) we self-consistently calculate effective masses,  $m_\eta^*(\vec{r})$  and  $m_{\omega_B}^*(\vec{r})$  at the position  $\vec{r}$  in the nucleus. Because the vector potentials for the same flavor of quark and antiquark cancel each other, the potentials for the  $\eta$  and  $\omega_B$  mesons are given respectively by  $m_\eta^*(r) - m_\eta$  and  $m_{\omega_B}^*(r) - m_{\omega_B}$ , where they will depend only on the distance from the center

Table 2: Parameters at the hadronic level (masses and coupling constants of mesons and photon for finite nuclei) [10].

field	mass (MeV)	$g^2/4\pi$ ( $e^2/4\pi$ )
$\sigma$	418	3.12
$\omega$	783	5.31
$\rho$	770	6.93
$A$	0	1/137.036

of the nucleus,  $r = |\vec{r}|$ . Before showing the calculated potentials for the  $\eta$  and  $\omega_B$ , we first show in Fig. 1 their effective masses and those calculated within an SU(3) quark model basis,  $\omega = \frac{1}{\sqrt{2}}(u\bar{u} + d\bar{d})$  (ideal mixing) and  $\eta_8 = \xi_8$  in Eq. (7), in symmetric nuclear matter. One can easily see that the effect of the singlet-octet mixing is negligible for the  $\omega_B$  mass in matter, whereas it is important for the  $\eta$  mass.

As an example, we show the potentials for the mesons in  $^{26}\text{Mg}$  and  $^{208}\text{Pb}$  in Fig. 2. Note that the actual calculations for  $^6\text{He}$ ,  $^{11}\text{B}$  and  $^{26}\text{Mg}$  are performed in the same way as for the closed shell nuclei,  $^{16}\text{O}$ ,  $^{40}\text{Ca}$ ,  $^{90}\text{Zr}$  and  $^{208}\text{Pb}$ . Although  $^6\text{He}$ ,  $^{11}\text{B}$  and  $^{26}\text{Mg}$  are not spherical, we have neglected the effect of deformation, which is expected to be small and irrelevant for the present discussion. (We do not expect that deformation should alter the calculated potentials by more than a few MeV near the center of the deformed nucleus, because the baryon (scalar) density there is also expected to be more or less the same as that for a spherical nucleus – close to normal nuclear matter density.) The depth of the potentials are typically 60 and 130 MeV for the  $\eta$  and  $\omega_B$  mesons, respectively, around the center of each nucleus. In addition, we show the calculated potentials using QMC-II [11] in Fig. 2, for  $^{208}\text{Pb}$ , in order to estimate the ambiguities due to different versions of the QMC model. At the center of  $^{208}\text{Pb}$ , the potential calculated using QMC-II is about 20 MeV shallower than that for QMC-I.

Now we are in a position to calculate single-particle energies for the mesons using the potentials calculated in QMC. Because the typical momentum of the bound  $\omega$  is low, it should be a very good approximation to neglect the possible energy difference between the longitudinal

and transverse components of the  $\omega$  [16]. Then, after imposing the Lorentz condition,  $\partial_\mu \phi^\mu = 0$ , solving the Proca equation becomes equivalent to solving the Klein-Gordon equation,

$$\left[ \nabla^2 + E_j^2 - m_j^{*2}(r) \right] \phi_j(\vec{r}) = 0, \quad (j = \eta, \omega_B), \quad (12)$$

where  $E_j$  is the total energy of the meson. An additional complication, which has so far been ignored, is the meson absorption in the nucleus, which requires a complex potential. At the moment, we have not been able to calculate the imaginary part of the potential (equivalently, the in-medium widths of the mesons) self-consistently within the model. In order to make a more realistic estimate for the meson-nucleus bound states, we include the widths of the  $\eta$  and  $\omega_B$  mesons in the nucleus by assuming a specific form:

$$\tilde{m}_j^*(r) = m_j^*(r) - \frac{i}{2} \left[ (m_j - m_j^*(r)) \gamma_j + \Gamma_j \right], \quad (j = \eta, \omega_B), \quad (13)$$

$$\equiv m_j^*(r) - \frac{i}{2} \Gamma_j^*(r), \quad (14)$$

where,  $m_j$  and  $\Gamma_j$  are the corresponding masses and widths in free space listed in Table 1, and  $\gamma_j$  are treated as phenomenological parameters to describe the in-medium meson widths,  $\Gamma_j^*(r)$ . According to the estimates in Refs. [7, 17], the widths of the mesons in nuclei and at normal nuclear matter density are  $\Gamma_\eta^* \sim 30 - 70$  MeV [7] and  $\Gamma_{\omega_B}^* \sim 30 - 40$  MeV [17], respectively. Thus, we calculate the single-particle energies for several values of the parameter,  $\gamma_j$ , which cover the estimated ranges.

From Table 1 and the calculated density distributions one can obtain the corresponding widths at normal nuclear matter density, as well as in the finite nuclei. Because of the recoilless condition for meson production in the GSI experiment [7, 8], we may expect that the energy dependence of the potentials would not be strong [18]. Thus we actually solve the following, modified Klein-Gordon equations:

$$\left[ \nabla^2 + E_j^2 - \tilde{m}_j^{*2}(r) \right] \phi_j(\vec{r}) = 0, \quad (j = \eta, \omega_B). \quad (15)$$

This is carried out in momentum space by the method developed in Ref. [19]. To confirm the calculated results, we also calculated the single-particle energies by solving the Schrödinger equation. Calculated single-particle energies for the  $\eta$  and  $\omega_B$  mesons, obtained solving the Klein-Gordon equation are respectively listed in Tables 3 and 4.

Table 3: Calculated  $\eta$  meson single-particle energies,  $E = \text{Re}(E_\eta - m_\eta)$ , and full widths,  $\Gamma$ , (both in MeV), in various nuclei, where the complex eigenenergies are,  $E_\eta = E + m_\eta - i\Gamma/2$ . See Eq. (13) for the definition of  $\gamma_\eta$ . Note that the free space width of the  $\eta$  is 1.18 keV, which corresponds to  $\gamma_\eta = 0$ .

		$\gamma_\eta=0$		$\gamma_\eta=0.5$		$\gamma_\eta=1.0$	
		$E$	$\Gamma$	$E$	$\Gamma$	$E$	$\Gamma$
$^{16}_\eta\text{O}$	1s	-33.1	0	-32.6	26.7	-31.2	53.9
	1p	-8.69	0	-7.72	18.3	-5.25	38.2
$^{40}_\eta\text{Ca}$	1s	-46.5	0	-46.0	31.7	-44.8	63.6
	1p	-27.4	0	-26.8	26.8	-25.2	54.2
	2s	-6.09	0	-4.61	17.7	-1.24	38.5
$^{90}_\eta\text{Zr}$	1s	-53.3	0	-52.9	33.2	-51.8	66.4
	1p	-40.5	0	-40.0	30.5	-38.8	61.2
	2s	-22.3	0	-21.7	26.1	-19.9	53.1
$^{208}_\eta\text{Pb}$	1s	-56.6	0	-56.3	33.2	-55.3	66.2
	1p	-48.7	0	-48.3	31.8	-47.3	63.5
	2s	-36.3	0	-35.9	29.6	-34.7	59.5
$^6_\eta\text{He}$	1s	-11.4	0	-10.7	14.5	-8.75	29.9
$^{11}_\eta\text{B}$	1s	-25.0	0	-24.5	22.8	-22.9	46.1
$^{26}_\eta\text{Mg}$	1s	-39.2	0	-38.8	28.5	-37.6	57.3
	1p	-18.5	0	-17.8	23.1	-15.9	47.1



Table 4: As in Tables 3, but for  $\omega$  meson single-particle energies. In the light of  $\Gamma$  in Refs. [17], the results with  $\gamma_\omega = 0.2$  are expected to correspond best with the experiment.

		$\gamma_\omega=0$		$\gamma_\omega=0.2$		$\gamma_\omega=0.4$	
		$E$	$\Gamma$	$E$	$\Gamma$	$E$	$\Gamma$
$^{16}_\omega\text{O}$	1s	-93.5	8.14	-93.4	30.6	-93.4	53.1
	1p	-64.8	7.94	-64.7	27.8	-64.6	47.7
$^{40}_\omega\text{Ca}$	1s	-111	8.22	-111	33.1	-111	58.1
	1p	-90.8	8.07	-90.8	31.0	-90.7	54.0
	2s	-65.6	7.86	-65.5	28.9	-65.4	49.9
$^{90}_\omega\text{Zr}$	1s	-117	8.30	-117	33.4	-117	58.6
	1p	-105	8.19	-105	32.3	-105	56.5
	2s	-86.4	8.03	-86.4	30.7	-86.4	53.4
$^{208}_\omega\text{Pb}$	1s	-118	8.35	-118	33.1	-118	57.8
	1p	-111	8.28	-111	32.5	-111	56.8
	2s	-100	8.17	-100	31.7	-100	55.3
$^6_\omega\text{He}$	1s	-55.7	8.05	-55.6	24.7	-55.4	41.3
$^{11}_\omega\text{B}$	1s	-80.8	8.10	-80.8	28.8	-80.6	49.5
$^{26}_\omega\text{Mg}$	1s	-99.7	8.21	-99.7	31.1	-99.7	54.0
	1p	-78.5	8.02	-78.5	29.4	-78.4	50.8
	2s	-42.9	7.87	-42.8	24.8	-42.5	41.9

Our results suggest one should expect to find bound  $\eta$ - and  $\omega$ -nuclear states as has been suggested by Hayano *et al.* [7, 8]. For the  $\eta$  single-particle energies, our estimated values lie between the results obtained using two different parameter sets in Ref [8]. From the point of view of uncertainties arising from differences between QMC-I and QMC-II, the present results for both the single-particle energies and calculated full widths should be no more than 20 % smaller in absolute values according to the estimate from the potential for the  $\omega$  in  $^{208}\text{Pb}$  in Fig. 2. Nevertheless, for a heavy nucleus and relatively wide range of the in-medium meson widths, it seems inevitable that one should find such  $\eta$ - and  $\omega$ -nucleus bound states. Note that the correction to the real part of the single-particle energies from the width,  $\Gamma$ , can be estimated nonrelativistically, to be of order of  $\sim \Gamma^2/8m$  (repulsive), which is a few MeV if we use  $\Gamma \simeq 100$  MeV.

In future work we would like to include the effect of  $\sigma$ - $\omega$  mixing, which (within QHD, at least) becomes especially important at higher densities [16]. It will also be important for consistency to calculate the in-medium width of the meson within the QMC model and to study the energy dependence of the meson-nucleus potential. While the energy dependence of the potential felt (for example) by the  $\omega$  may be quite significant as we move from a virtual  $\omega$  ( $q^2 \sim 0$ ) to an almost real  $\omega$  ( $q^2 \sim m_\omega^2$ ) [17], QHD studies in nuclear matter did not reveal a strong energy dependence for  $q^2$  near  $m_\omega^2$  [16] – the region of interest here. Nevertheless, this point merits further study in finite nuclei and within QMC itself.

To summarize, we have calculated the single-particle energies for  $\eta$ - and  $\omega$ -mesic nuclei using QMC-I. The potentials for the mesons in the nucleus have been calculated self-consistently in local density approximation, embedding the MIT bag model  $\eta$  and  $\omega$  mesons in the nucleus described by solving mean-field equations of motion. Although the specific form for the widths of the mesons in medium could not be calculated in this model yet, our results suggest that one should find  $\eta$ - and  $\omega$ -nucleus bound states for a relatively wide range of the in-medium meson widths. In the near future, we plan to calculate the in-medium  $\omega$  width self-consistently in the QMC model.

## Acknowledgment

We would like to thank S. Hirenzaki, H. Toki and W. Weise for useful discussions. Our thanks

also go to R.S. Hayano for discussions at the *2nd International Symposium on Symmetries in Subatomic Physics* held at University of Washington, Seattle, June 25 – 28, 1997, which triggered the present work, and for providing us the experimental proposal, Ref. [7]. This work was supported by the Australian Research Council.

## References

- [1] Quark Matter '97, to be published in Nucl. Phys. A (1998).
- [2] P. Wurm for the CERES collaboration, Nucl. Phys. A 590 (1995) 103c.
- [3] M. Masera for the HELIOS collaboration, Nucl. Phys. A 590 (1995) 93c.
- [4] G.Q. Li, C.M. Ko and G.E. Brown, Nucl. Phys. A 606 (1996) 568; G. Chanfray, R. Rapp and J. Wambach, Phys. Rev. Lett. 76 (1996) 368.
- [5] M. Kossov *et al.*, TJNAF proposal PR-94-002 (1994); P.Y. Bertin and P.A.M. Guichon, Phys. Rev. C 42 (1990) 1133.
- [6] HADES proposal, see HADES home page: <http://piggy.physik.uni-giessen.de/hades/>; G.J. Lolos *et al.*, Phys. Rev. Lett. 80 (1998) 241.
- [7] R.S. Hayano *et al.*, proposal for GSI/SIS, September, 1997; R.S. Hayano, 2nd Int. Symp. on Symmetries in Subatomic Physics, Seattle (1997); R.S. Hayano and S. Hirenzaki, contributed paper to *Quark Matter '97*, Tsukuba (1997); T. Yamazaki *et al.*, Z. Phys. A 355 (1996) 219.
- [8] R.S. Hayano, S. Hirenzaki and A. Gillitzer, nucl-th/9806012.
- [9] P.A.M. Guichon, K. Saito, E. Rodionov and A.W. Thomas, Nucl. Phys. A 601 (1996) 349.
- [10] K. Saito, K. Tsushima and A.W. Thomas, Nucl. Phys. A 609 (1996) 339.
- [11] K. Saito, K. Tsushima and A.W. Thomas, Phys. Rev. C 55 (1997) 2637; K. Tsushima, K. Saito, A.W. Thomas and S.W. Wright, Phys. Lett. B 429 (1998) 239.
- [12] P.A.M. Guichon, Phys. Lett. B 200 (1988) 235.

- [13] H.Q. Song, R.K. Su, Phys. Lett. B 358 (1995) 179; P.G. Blunden and G.A. Miller, Phys. Rev. C 54 (1996) 359; X. Jin and B.K. Jennings, Phys. Lett. B 374 (1996) 13; H. Müller and B.K. Jennings, Nucl. Phys. A 626 (1997) 966; R. Aguirre and M. Schvellinger, Phys. Lett. B 400 (1997) 245; P. K. Panda, A. Mishra, J. M. Eisenberg and W. Greiner, Phys. Rev. C 56 (1997) 3134; H. Müller, Phys. Rev. C57 (1998) 1974.
- [14] B.D. Serot and J.D. Walecka, Adv. Nucl. Phys. 16 (1986) 1.
- [15] Review of Particle Physics, Phys. Rev. D 54 (1996) 1.
- [16] K. Saito, K. Tsushima, A.W. Thomas and A.G. Williams, Phys. Lett. B 433 (1998) 243.
- [17] B. Friman, nucl-th/9801053; F. Klingl and W. Weise, hep-ph/9802211.
- [18] T. Waas, R. Brockmann and W. Weise, Phys. Lett. B 405 (1997) 215; T. Yamazaki *et al.*, Phys. Lett. B 418 (1998) 246.
- [19] D.H. Lu and R.H. Landau, Phys. Rev. C 49 (1994) 878; Y.R. Kwon and F. Tabakin, Phys. Rev. C 18 (1978) 932; R.H. Landau, *Quantum Mechanics II* (John Wiley & Sons, New York, 1990).

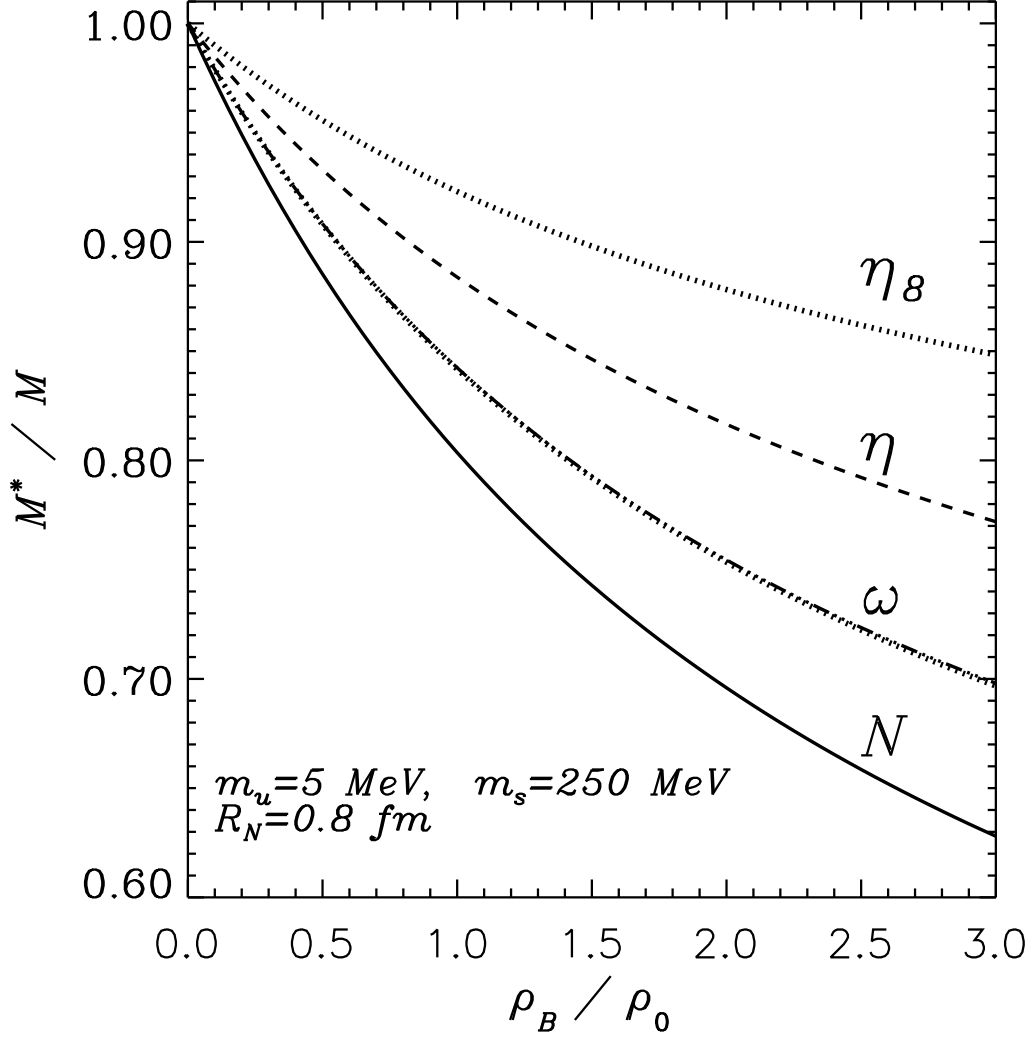


Figure 1: Effective masses of the nucleon, physical  $\eta$  and  $\omega$  mesons, and those calculated based on SU(3) quark model basis (the dotted lines), namely  $\omega = \frac{1}{\sqrt{2}}(u\bar{u} + d\bar{d})$  (ideal mixing) and  $\eta_8 = \frac{1}{\sqrt{6}}(u\bar{u} + d\bar{d} - 2s\bar{s})$ . The two cases for the  $\omega$  meson are almost degenerate. (Normal nuclear matter density,  $\rho_0$ , is  $0.15 \text{ fm}^{-3}$ .)

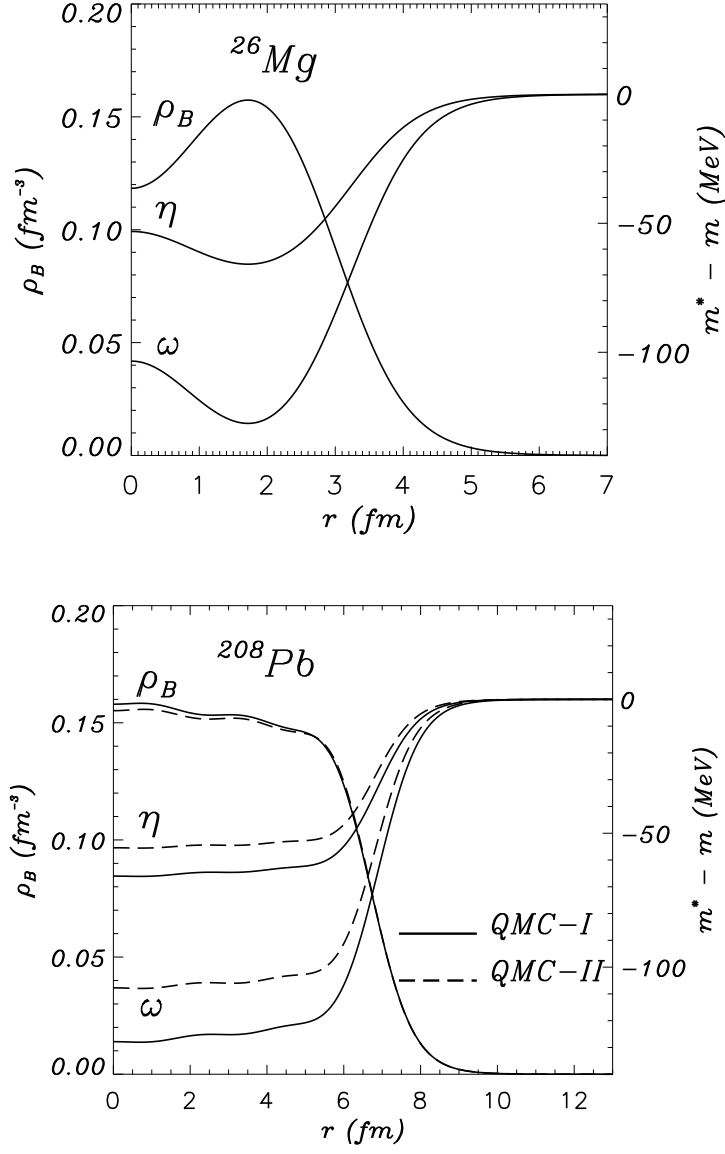


Figure 2: Potentials for the  $\eta$  and  $\omega$  mesons,  $(m_\eta^*(r) - m_\eta)$  and  $(m_{\omega_B}^*(r) - m_{\omega_B})$ , calculated in QMC-I for  $^{26}\text{Mg}$  and  $^{208}\text{Pb}$ . For  $^{208}\text{Pb}$  the potentials are also shown for QMC-II.